

GALAXY AND HALO ROOT SYSTEMS: FINGERPRINTS OF MASS ASSEMBLY

MARK NEYRINCK 

Blue Marble Space Institute of Science, Seattle, WA 98104, USA

MIGUEL ARAGÓN-CALVO

UNAM, Universidad Nacional Autónoma de México, Instituto de Astronomía, AP 106, Ensenada 22800, BC, México

ISTVÁN SZAPUDI

Institute for Astronomy, University of Hawaii, 2680 Woodlawn Drive, Honolulu, Hawaii, 96822, USA

Version March 28, 2025

Abstract

We discuss what we call halo or galaxy root systems, collections of particle pathlines that show the infall of matter from the initial uniform distribution into a collapsed structure. The matter clumps as it falls in, producing filamentary density enhancements analogous to tree roots and branches, blood vessels, or even human transportation infrastructure in cities and regions. This relates to the larger-scale cosmic web, but is defined locally about one of its nodes; a physical, geometric version of a merger tree. We find dark-matter-halo root systems on average to exhibit more roots and root branches for the largest cluster haloes than in small haloes. This may relate to the ‘cosmic-web detachment’ mechanism that likely contributes to star-formation quenching in galaxy groups and clusters. We also find that high spin manifests in these root systems as curvier roots.

1. INTRODUCTION

The cosmic web (Bond *et al.* 1996) is the branching network of matter that weaves throughout the Universe, connecting galaxies on intergalactic scales. Branching networks with similarities to the cosmic web abound on much smaller scales in nature too, visible on Earth in more familiar systems: river networks; infrastructure networks of cities and regions; trees, roots, and mycelial networks; fracture networks; and even circulatory, respiratory and neural systems in our bodies.

There is some understanding of why these systems in many cases look similar, and even artistic modes of knowing have aided in this; for example, room-sized art installations by Tomás Saraceno based on spiderwebs (Ball 2017) inspired the finding that the cosmic web is a structural-engineering spiderweb (a network of links that can be all in tension, or all in compression) (Neyrinck *et al.* 2018). Some neural networks look similar to the cosmic web, as well (Vazza and Feletti 2020). Art has encouraged efforts to understand that correspondence (Neyrinck *et al.* 2020), including a tentative finding that local cosmic webs, just like neurons (Cuntz *et al.* 2010), and urban transportation networks (Leite and De Bacco 2024), balance the efficiency of minimal-spanning trees with as-direct-as-possible transport to a single hub. Measurements of branching systems are obviously of use for medical-imaging diagnosis; for example, the fractal dimension of the bronchial lung structure is of diagnostic use (Tanabe *et al.* 2020). All of these networks have differences as well as similarities, obviously, and identifying or falsifying connections helps to understand how they work.

One rigorous similarity between trees and cosmic webs is already known: trees are often structural spiderwebs (in equilibrium if entirely in compression), and therefore share geometric underpinnings with the cosmic web. But an obvious difference between a tree and the cosmic web is that trees are compact, with a single branch. The cosmic web, on the other hand, is in principle an infinite, percolating structure (if observed on a constant, recent timeslice). But locally, cosmic-web patches around haloes can resemble trees. This resemblance strengthens if we look at the accretion pattern that underlies a halo.

We call the web formed by matter as it collapsed in the past into a halo or galaxy a *root system*. In this introductory work, we just analyze haloes, but also touch on what we expect for galaxy root systems. A root system is a projection of a halo through time, instead of space; it is the projected ensemble of matter trajectories, or pathlines, for all particles that end up in the halo. Pathlines are common concepts in fluid mechanics, so it might seem that we are making an unduly big deal out of this. But a couple of choices make it particularly interesting, to our knowledge not explored

before, cosmologically: (1) we view it in comoving coordinates, so infall dominates other motions; and (2) we subtract off any halo bulk motions that might obscure the infall pattern; we keep the centroid of the protohalo that eventually forms the halo in the same place at each snapshot that we use to render it.

An essential concept in galaxy formation is a galaxy or halo merger tree (e.g. [Srisawat et al. 2013](#)), which should usually correspond closely to the root systems we define. But ‘tree’ in ‘merger tree’ refers to the abstract computer-science concept of nodes in a hierarchy, rather than a physical geometric branching structure.

There is also a link between root systems and ‘watershed superclusters’ or ‘basins of attraction,’ such as Laniakea ([Tully et al. 2014](#); [Dupuy and Courtois 2023](#); [Valade et al. 2024](#)), defined by dominantly inward flows. Without the structure-freezing effect of a cosmological constant, a watershed supercluster would eventually form a giant halo, and so streamlines of reconstructions of the velocity field in such a region (e.g. [Hoffman et al. 2024](#)) would approximate that halo’s root system.

1.1. Galaxies and cities

A transportation network along roads into a region is a branching system, e.g. the ‘Major flows by truck in and out of Texas, 2010’ shown in Chapter 7 of [West \(2017\)](#), which has a direct analogy to the root systems we show here. A key motivation for our study is the recent growth of urban science, i.e., the science of cities, especially their intriguing scaling laws that are closely tied to infrastructure networks. ([Bettencourt 2013, 2021](#)).

Larger cities have been measured to have higher ‘productivity’ per capita than less-populous cities. Productivity here encompasses things that benefit from interpersonal interaction, such as gross domestic product, patents, or academic papers, and also unpleasant things like traffic and housing prices. But they also have more efficient infrastructure, i.e. less infrastructure per capita. For example, the the total street length per capita is smaller in a big city. The scaling of productivity P with population N is measured to take the approximate form $P(N) \propto N^{1+\delta}$, for $\delta \approx 0.2 > 0$. Intriguingly, the infrastructure scales in an opposite, related way; $I(N) \propto N^{1-\delta}$. The sophisticated infrastructure tends to put more people in contact with each other, in a ‘productive’ way.

Might this relate at all to galaxies or haloes? A halo root system is a sort of ‘infrastructure.’ But it is (approximately, at least) a hierarchical tree; as apparently needed stating, well before the concept of fractals, ‘a city is not a tree’ ([Alexander 1965](#)). This means that nodes of interaction in a city do not form a strict hierarchical tree; nodes in a city have connections of various kinds, far across the city, as well as nearby.

Still, it is interesting to ponder what might be the ‘productivity’ of a galaxy, in analogy to a city. Star formation? Energy dissipation? Galaxies and the structures inside them are examples of dissipative structures ([Nozakura and Ikeuchi 1984](#)), so energy dissipation and entropy production might be viewed as a ‘product’ of a galaxy.

We leave these questions hanging for now, but after introducing a 2D example, and then discussing our methods and results, will return to them in the discussion.

1.2. A 2D Illustration

Even if there can be essential differences between a 2D and the actual 3D universe, it is often instructive to start with a 2D version of a 3D process. Fig. 1 shows halo root systems from a 2D N -body simulation with 256^2 particles. We used the python code of [Hidding \(2020\)](#), with its default settings (a box size of 50 Mpc/h, a power-law power spectrum with slope $n = 1/2$), and for dynamical simplicity, an Einstein-de Sitter expansion history.

For halo-finding in the final snapshot, we used a simplification of the ORIGAMI ([Falck et al. 2012](#)) algorithm, entirely coded in python. We tagged particles which differed in their place in line (lines being rows and columns along the axes, and 45°-diagonals), comparing initial and final orderings. The ORIGAMI morphology was the number of orthogonal axes in which a particle was tagged as out-of-order; a halo particle has crossed along two axes. This only required comparison of ordered to ‘argsort’ arrays in each row and column, extremely fast. However, this simple method misses some crossings, because assuming that orderings become randomized in a collapsed structure, there is some chance of a particle happening to recover its initial place in line. So, there were holes of untagged particles in collapsed patches; we filled these minimally, with the scikit-image ([van der Walt et al. 2014](#)) ‘morphology.remove_small_holes’ function. We then defined haloes as contiguous sets of halo particles in Lagrangian coordinates; note that this contrasts with below findings about streaks originating far outside haloes.

2. METHOD

We measured root systems from ‘final’ (redshift $z = 0$) friends-of-friends haloes in an IllustrisTNG simulation ([Pillepich et al. 2018](#); [Nelson et al. 2019a,b](#)), to enable us to study correlations between their properties and the plentiful measurements that are readily accessible in the IllustrisTNG database at <https://www.tng-project.org/>. For each of the 100 snapshots from initial to final conditions, we binned all particles that end up in a final halo into cells, keeping the halo or protohalo centroid in the center.

Our main root-system measurements are from the 540^3 -particle TNG50-3-Dark simulation, with box length 35 Mpc/h, with the same initial fluctuations as in the TNG50-3 simulations with the TNG galaxy-formation model. It has a concordance set of cosmological parameters specified by the [Planck Collaboration et al. \(2015\)](#). The size of this simulation in particle number is modest, but rendering root systems is unfortunately rather time-consuming from these simulations; matches must be found between particle IDs in particular haloes and particles in all files at all snapshots;

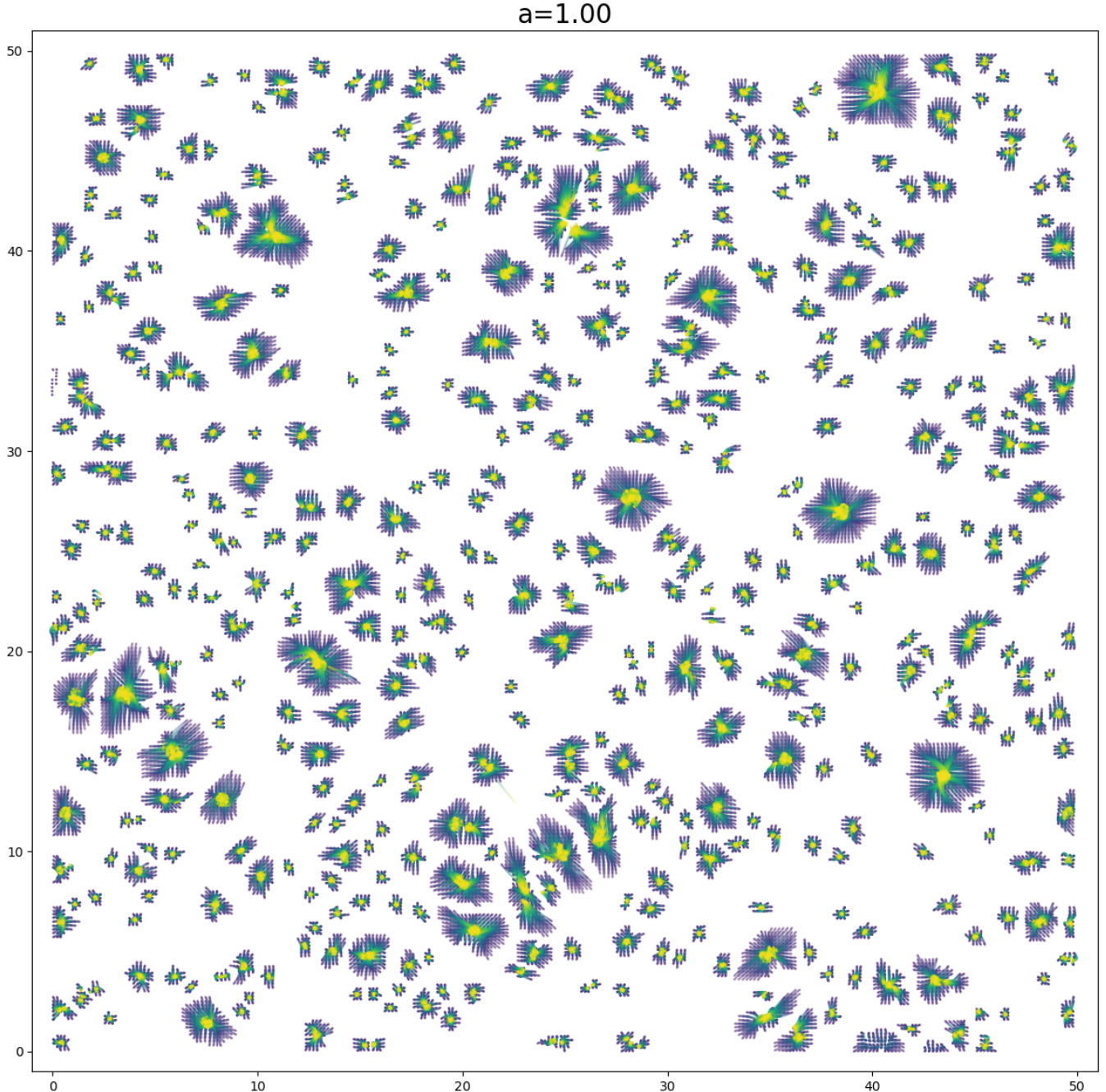


FIG. 1.— Halo root systems in a 2D N -body simulation. At each timestep rendered, the particles are recentered to retain their Lagrangian (initial) centroids, removing the effect of bulk flows. Lagrangian outskirts of haloes, from the initial few snapshots, are in purple. Particles are rendered with increasing yellowness and decreasing opacity with time, until their final form appears in yellow. Roots appear in greenish colors, rendered at intermediate times. The periodic boundary conditions inform halo membership, but not pathlines, some of which jump across the edges. An animation of the particle deposition with time is at <https://neyrinck.github.io/haloroots2d.mp4>.

it took ~ 2 days to render 1000 halo root systems. To study resolution effects, we also rendered some haloes from TNG50-2-Dark, with $8\times$ mass resolution; each halo indeed took $\sim 8^2\times$ longer.

We rendered the simulations in $1.5 \text{ Mpc}/h$ and $0.75 \text{ Mpc}/h$ boxes with 128^3 voxels. We deposited particles using the ‘nearest-grid-point’ method, i.e. binning with a simple histogram, weighting each particle by half the cosmic time between adjacent snapshots. There were enough snapshots that there was visually negligible particle discreteness noise in this, but if fewer snapshots were available, it would make sense to draw lines between particles instead of just depositing their mass.

3. RESULTS

We show projected root systems for 25 haloes in Fig. 2, spanning ranges of mass and halo spin. Each row represents a mass bin; within that, columns show haloes of increasing final spin in the mass bin, from minimum to maximum. We measured ‘spin’ as the magnitude of the total angular momentum, summed with a cross product of $z = 0$ particle displacements and velocities away from the halo’s position and velocity centroids. For this simple but not dimensionless spin parameter L , we observed a trend $L \propto M^{\sim 1.5}$, roughly that seen previously (e.g. Heavens and Peacock 1988; Neyrinck *et al.* 2020); to eliminate bias from this trend within a mass bin, we actually ranked the quantity $(L/M^{1.5})$.

The outer boundaries of the root systems are essentially their Lagrangian protohaloes, i.e. the set of initial-conditions uniform-density space that collapses to form the halo. This is because, in comoving coordinates, infalling particles move toward the centroid, and generally come to occupy space where another particle used to be. But it is only ‘essentially’ so because this has exceptions; the root system also includes particle pathline streaks between any disconnected regions of the Lagrangian protohalo and its centroid.

Animations of root systems’ rotating 3D structure can be found at https://neyrinck.github.io/halo_gif_table.html, showing the 100 haloes with the highest mass, https://neyrinck.github.io/halo_gif_table_skip10.html, showing every 10th of the 1000 highest-mass haloes, and https://neyrinck.github.io/halo_gif_spin_table.html, showing the same grid as appears in Fig. 2. For these, we rendered the haloes with 10 equally-spaced contours of the log-density up to the maximum, with increasing opacity.

A first finding is the surprising (to us) prevalence of streaks reaching far outside of a convex shape. We emphasize though that we expect this to depend on the halo finder and definition; we used haloes defined by a standard Friends-of-Friends method. In this, particles within a physically motivated linking length of each other are grouped together as a halo. This is a conveniently simple definition, but it does not enforce that the haloes are physically persistent through time; it does not, in particular, include an ‘unbinding’ step which removes particles not gravitationally bound to the halo. Although for our purposes, an alternative halo definition may have been more sensible (see, e.g., Knebe *et al.* 2011), we used FOF haloes since they underly most quantities in the TNG database.

Why are there so many such streaks? For this to happen, particles originating far away enter the halo, but nearer particles along or near the streak strangely do not. Perhaps the faraway particles participated in few-body interactions that took them into the halo, bypassing the intervening particles. Perhaps these are particles that were once in one halo, but swapped into another inside a structure like a filament. As we see below in Fig. 4, these streaks largely persist at higher resolution, and so seem to be physically real. At least one of us has worked on defining haloes as hole-free regions of Lagrangian space, which seems reasonable, but maybe that definition has physical (instead of numerical) exceptions that these results illustrate. Protohaloes may even be idealized to have nearly convex protohalo shapes, even though they are known not always to be so (Ludlow and Porciani 2011). Also, it is not obvious in the root system, but in the initial snapshot, most Lagrangian protohaloes were not quite single blobs topologically, with some gaps of particles just inside their outer boundaries. Perhaps at the final snapshot, these particles are in ‘backsplash regions’ that have already passed through the halo center, and are then lingering at the turnaround radius, not meeting the density criterion to be linked.

3.1. Root-system complexity

We define a *root* as an accumulation of pathlines in the root system, that appear roughly as cosmic-web filaments (nearly 1-dimensional curves). Because it is ambiguous how physically relevant the streaks are that poke out of the central protohalo (the nearly convex shapes of nearly uniform background density), we concentrate attention on roots inside that central protohalo.

A quick visual impression finds more ‘structure’ (more roots, and more branching) in a high-mass halo than a low-mass one. This is suggestive of the findings of Galárraga-Espinosa *et al.* (2023): the number of filaments around a high-mass galaxy is generally higher than around a low-mass one (see also Aragón-Calvo *et al.* (2010a) for similar findings for clusters), in this same TNG50 simulation. If major roots of the root system correspond to filaments outside the halo after it has formed, these may be very related findings.

Also, based just on a visual impression, we find that the roots in a high-spin root system are generally more curved, or tortuous (a word used to describe a curvy river system, not to be confused with ‘torturous’). Some even have a gap at the center between two blobs. This could happen if the blobs are linked in the FOF method, but have not yet physically merged. This is entirely expected; although halo spin may ultimately be sourced by extended regions of the initial velocity field (Neyrinck *et al.* 2020), this may often manifest as a merger of haloes in spiraling orbits.

However, although most of this paper is about the roots, the most visually striking aspects of the root systems, there is a substantial background of matter in them, as well. A fair fraction of matter seems to come straight into the halo, without noticeably clumping.

We would like to undertake a comprehensive study of the abundance, structure, and branching of halo roots, as has occurred in other disciplines. Many branching structures have objective boundaries, such as cell walls for neurons, blood-vessel boundaries for the circulatory system, bronchial boundaries in the lungs, road edges for transportation, or river banks for river networks. Given their clear medical value, blood-vessel analysis algorithms (e.g. the review Moccia *et al.* 2018) have matured for decades, and even inspired cosmic-web analysis (Aragón-Calvo *et al.* 2007).

But a difficulty for this application is that there is no ground truth of what is a root and a root boundary; all we have immediate access to with dark matter is density contrasts of varying strength. In the case of the usual cosmic web, dynamical information such as particle crossings are of help to objectively define some structures (Falck *et al.*

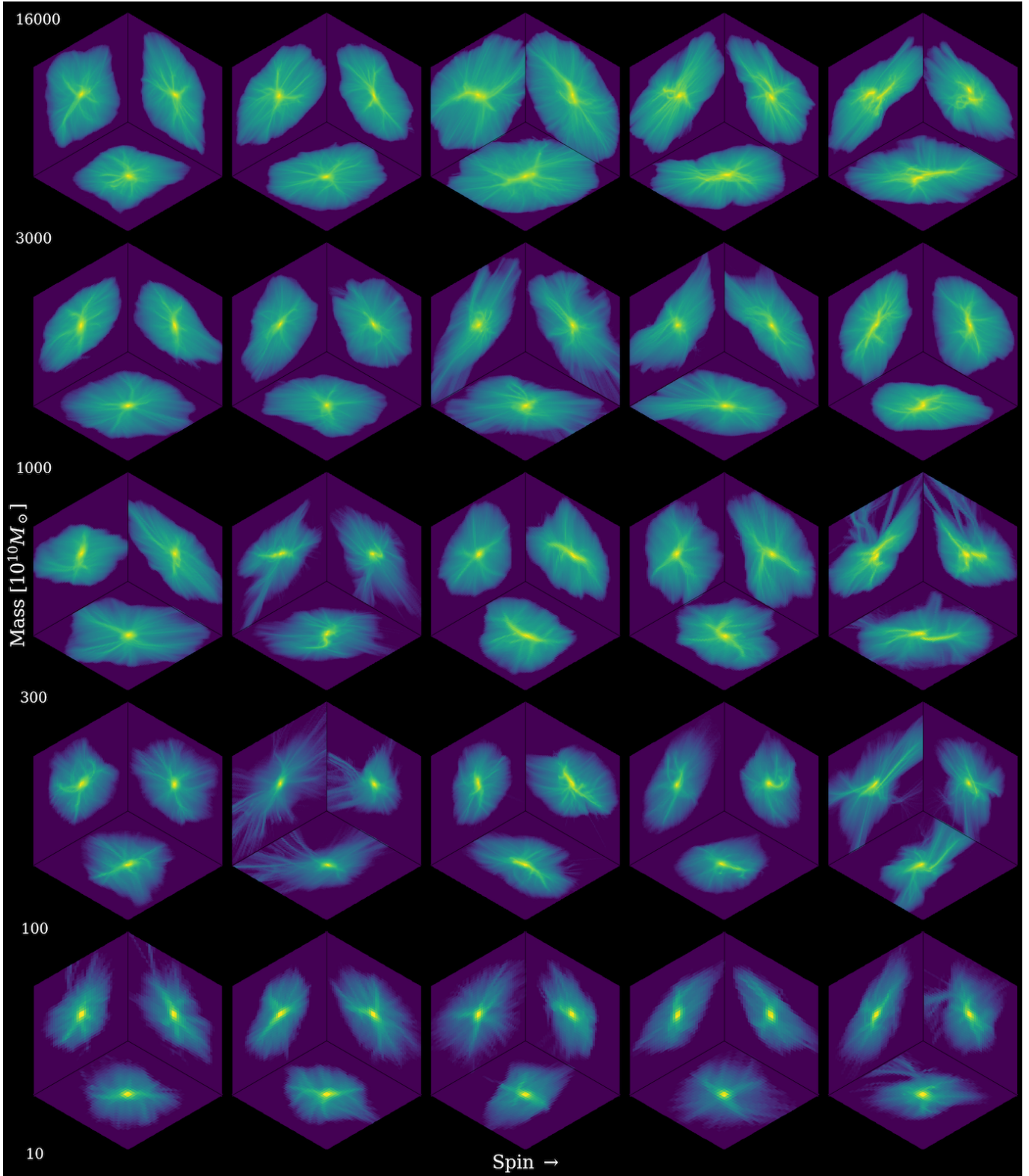


FIG. 2.— Projected halo root systems (HRS) spanning ranges of mass and final halo spin. Each hexagonal panel shows the log-density of 3 projections along the cardinal axes of the rendered cube, scaled to be of side length $0.8V_{\text{HRS}}^{1/3}$, where V_{HRS} , roughly proportional to the mass, is the number of nonzero-density voxels in the HRS. Deep purple indicates 0; bright yellow indicates the maximum, typically $\sim 2 \times 10^5$ deposited particles (bottom row), up to $\sim 1.2 \times 10^6$ (top row). Mass bin edges (in units of $10^{10} M_{\odot}$) of each row are shown at left. The top row shows galaxy-cluster-size haloes, containing hundreds of galaxies each, according to the TNG model. By the second-to-last and last rows, some haloes contain only a single galaxy. In columns, haloes in that bin are shown as close as possible to the minimum, 25th percentile, median, 75th percentile, and maximum spin.

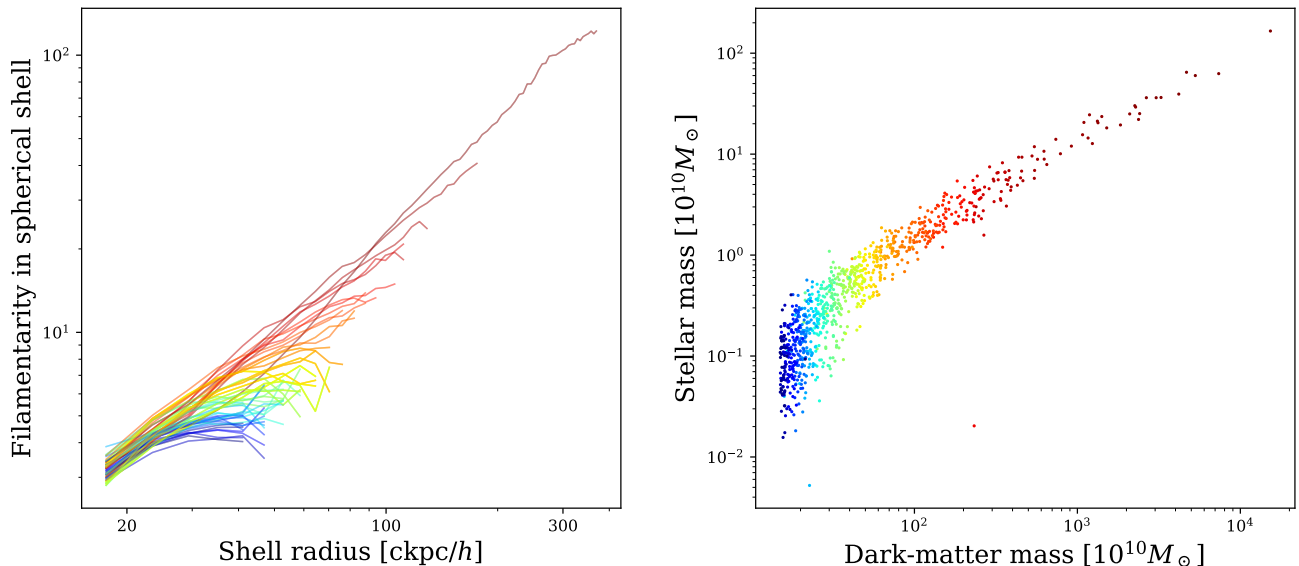


FIG. 3.— *Left*: Filamentarity in spherical shells as a function of radius from the halo root system centroid, for the 1000 most massive haloes in TNG50-3-Dark, averaged in 20-halo mass bins. ‘Filamentarity’ here means the blobbiness- and density-weighted number of filaments found by a 2D Hessian-based blob finder, described in the Appendix. The lowest radius shown corresponds to only 3 pixels, and the upper radius to the half-radius of the box, 63 pixels. As halo mass increases, the filamentarity generally increases at a given radius and there is a reduced filamentary downturn at the edge of the halo root system. This is consistent with the visual impression that the halo root systems do not have similar structure across mass; the number and branching of filaments increases with mass. Here, ‘ckpc’ means comoving kiloparsec, used to remind the reader that the root systems are projected in comoving coordinates. *Right*: The dark-matter and stellar masses of these haloes, colored the same way as at left.

2012). Similarly, we imagine that tagging particle-trajectory crossings could define roots objectively and decisively. Referencing the origami concept (Neyrinck 2015a), because the root systems show the infall of all particles, the roots are essentially creases in a fabric, where an initially uniform, uncreased 3D patch of the universe bunches together.

The galaxy root system built from pathlines of gas that ultimately forms stars (Aragon-Calvo *et al.* 2014) we expect would have more objective boundaries, as well. In that paper, infalling gas, colored according to the time that gas ultimately would form stars in a galaxy, seems to form a branching structure; see the upper-right panel of its Fig 1. Unfortunately in IllustrisTNG, analyzing gas infall would be much more difficult than dark matter infall, since in Arepo (Weinberger *et al.* 2020), gas particles are tracers, not representing the same matter throughout the simulation. They do not precisely go with the flow, and gas can flow through gas-cell walls. It may be possible to do this star-forming gas tracking (a paper addressing this sort of thing is Genel *et al.* 2013), but this is too large a task for the present.

As a first quantitative measurement of the root systems, we use a multiscale ‘blob’ finder (where a blob is roughly circular) on spherical shells in voxel-length radius increments from the root-system centroid. Instead of making a decisive cut for each blob as to whether it counts as a root or not, we sum up a probabilistic field that quantifies blobbiness. We would like to detect clear branching events as well in the root system, but this probabilistic summing makes that more challenging. The Appendix contains details of this procedure, and Fig. 3 shows the results.

At fixed shell radius, from $r \sim 30\text{--}80$ ckpc/h, the filamentarity generally goes up with halo mass. More interestingly, the filamentarity generally increases with radius for a given curve (corresponding to a single 20-halo mass bin). The slope of the upper limit of the curves is $f \propto r^1$, which is a substantial rise, but it rises slower than the surface area of the shell ($\propto r^2$), which might be the expected rise if the blob-finding were due to noise. The rise suggests branching, since new roots arise at larger radius. This rise persists throughout the range of radius for high-mass haloes, but it turns over for lower-mass haloes, indicating less branching in these root systems.

3.2. Root systems and cosmic-web detachment

Fig. 3 also shows a plot of the dark-matter and stellar masses for these haloes, as reported in the TNG database. We did this because one motivation for our root-system study is the cosmic-web detachment (CWD; Aragon Calvo *et al.* 2019) mechanism for external star-formation quenching that some of us proposed. ‘Quenching’ refers to a drastic, possibly sudden reduction in the star-formation rate. High-mass galaxies and clusters are often quenched; here, this appears as a reduction in the slope of the stellar mass to dark-matter-halo mass relation at high mass.

The CWD mechanism is as follows: when haloes first form (from infall rather than mergers), they are generally surrounded by primordial filaments, along which gas and dark matter enter the halo, ultimately forming stars. These are halo roots in the present picture. The ‘web detachment’ occurs when these roots get ‘detached,’ or disrupted, which may through a merger with another halo, or with a filament – in the CWD paper, we quantified these detachment events with stream crossing on larger scales than the primordial haloes.

Because the halo root system is a single 3D representation of a halo merger tree, these CWD events should often show

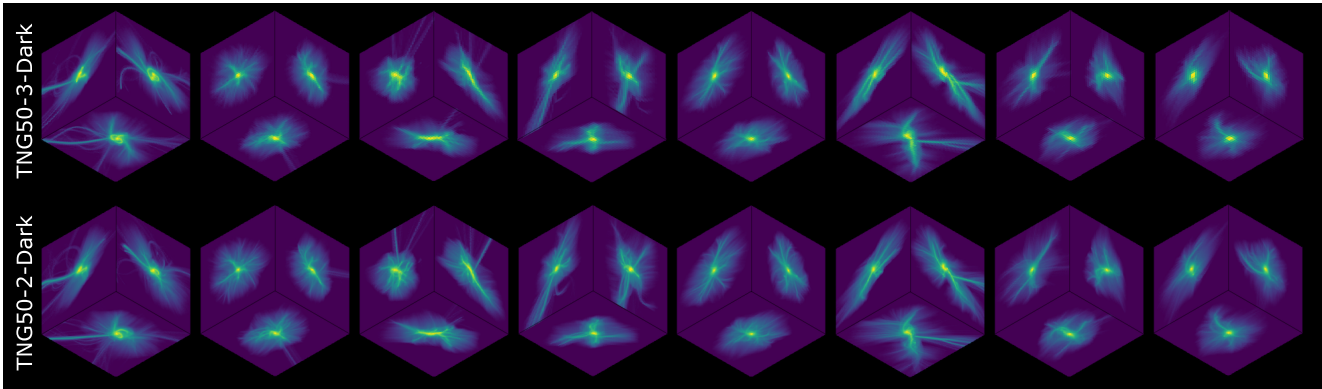


FIG. 4.— Comparison between projected root systems, as in Fig. 2, for 8 haloes in TNG50-3-Dark (top row), and the same haloes with $8\times$ higher mass resolution in TNG50-2-Dark, with twice as many voxels in each dimension (bottom row). They are the 250th, 350th ... to the 950th most massive in TNG50-2-Dark, and range in mass from 1.4×10^{11} to $8.3\times 10^{11}M_{\odot}$. Haloes in each pair look quite similar, but there are small differences.

up in the root system as major root branchings. Our measurements of high root-system filamentarity and branching prevalence for the largest haloes suggests that we are seeing that. Visual inspection of many of the high-mass root systems only reveals a few major branchings, but the background appearance reminds us of a corrugation; that may indicate many small branchings into small tributary subhaloes.

So, we suggest that here that the increased branching in larger-mass haloes is a signal that some cosmic-web detachment is going on, and plays a role in quenching star formation in these haloes.

However, the star-formation picture in the TNG model includes many processes internal to galaxies that are explicitly stochastic; in neither the simulation nor in nature would we expect CWD to completely determine, or even be the primary cause of star-formation quenching. Indeed, any simulation that aims to produce galaxy observables from a fixed set of initial conditions is best viewed as a particular realization of a probabilistic ensemble (Genel *et al.* 2019), whether the stochasticity that produces that probability distribution is epistemic (simply a necessity of finite resolution), or ontic/ontological (arising from true stochasticity not present in the initial-conditions density field) (Neyrinck *et al.* 2022). Still, we expect that deterministic external mechanisms such as CWD might show up somehow in halo root systems. For the largest cluster haloes, containing hundreds of galaxies, the difficulty of fresh star-forming gas mechanically finding its way into galaxies is undeniable, but other mechanisms could dominate quenching at lower mass, internal, apparently stochastic processes such as AGN, without obvious indications in the halo or galaxy root system.

3.3. Resolution effects

An effect that could artificially mimic our claimed reduced number and branching of roots in lower-mass halo root systems is if we were smearing over structure at lower mass. This could either come from too-low simulation mass resolution (too few particles per halo), or with too-big fixed-size voxels. The number of particles in the lowest-mass halo we investigate is 6739, which seemed adequate to us, but it is still worth checking what would happen with increased resolution.

To study whether this is the case, in Fig. 4 we show 8 halo root systems from our fiducial TNG50-3-Dark simulation, each side-by-side with halo root systems with 8 times more particles.

We note also that it is not precisely accurate to call these the ‘same haloes’ simulated with different resolutions, because the haloes in the higher-resolution simulation are not only built in the initial conditions from $8\times$ the particles, but additional small-scale structure from $8\times$ the Fourier modes. Given this, the changes in the root system may seem remarkably small; the reason for this is that the power spectrum is steeply declining with wavenumber in the regime of the added modes.

Another not-entirely-expected finding from this crude resolution study is that the externally arriving streaks that occur in many of these halo root systems are generally present (with some fluctuations in their density) in both simulations, supporting the view that they are physical instead of numerical.

In general, the appearance of each projected halo seems to have modest dependence on resolution. In particular, we conclude that there does not seem to be a substantial increase in the number of ‘roots’ in these smaller haloes at higher resolution.

4. DISCUSSION

Our finding that the abundance and branching of roots increases in a larger-mass halo might have several implications. It may be associated with the finding that the number of galaxies in a large-mass halo is much larger than in a small halo; the cluster-sized haloes in the top row of Fig. 2 contain hundreds of galaxies, as determined by the TNG star-formation model. In cosmology, it is tempting to consider halo structure to be weakly dependent on scale, and for a

wide variety of subhaloes to be possible galaxies (e.g. Moore *et al.* 1999). Various plausible mechanisms have been proposed to explain an effective physical smoothing that produces galaxies only in the largest subhaloes. But maybe the difference in structure in low and high-mass root systems could illustrate a partial explanation in the dark matter dynamics, as well.

The cosmic-web context of the haloes is also important to consider; the largest, cluster-size haloes occupy the largest nodes of the cosmic web. Lower-mass haloes, on the other hand, can occupy a variety of cosmic-web environments. If they are in a large void, they may have rather undisturbed accretion along scaled-down filaments. But if they are in a filament or wall (i.e. their primordial webs are ‘detached’), their dynamics become more enmeshed with their surroundings. Because filaments form in particular tidal environments that persist throughout cosmic time, the roots of a particular halo are likely to align with filaments outside the halo. Looking at how root systems depend on cosmic-web environment is a clear avenue to follow up.

4.1. Galaxy information

Root systems give a visual, geometric representations of the accretion, infall, or merger history in a halo (or galaxy). Thus, we assert that they summarize the influence that large-scale-structure dynamics can possibly have over goings-on inside a halo. This patch of all the matter that, through physical flows, could have causally affected a halo and galaxies within it has been called the *matter horizon* (Ellis and Stoeger 2009). This horizon is much nearer than cosmological event or particle horizons, but it dominates the causal influence among parts of the light cone. Influences from outside the matter horizon are not impossible. Any tiny perturbation, through chaos, might eventually have some effect on galaxy scales on a dynamical timescale, extrapolating from other turbulent systems (Bandak *et al.* 2024). One mechanism of affecting a galaxy from outside the matter horizon is (e.g. ultraviolet) light from another galaxy that ionizes gas. But otherwise, a substantial perturbation from outside the matter horizon also requires substantial imagination. For example, a ridiculous possibility would involve life: a maximally advanced civilization could in principle either produce, or not, a substantial perturbation in a galaxy (diverting a star into a central black hole?) based on the results of some cosmological-scale astronomical observation.

One of us suggested that the initial density field within the Lagrangian patch that collapsed to form a halo quantifies the information available to form it (Neyrinck 2015b). In principle, the initial velocity field within that patch should carry similar information as in halo root system. But we find the root system to be particularly visually comprehensible, and to display features such as mergers directly. As we commented in §3.3, it is interesting that small-scale velocity modes have little influence on the root system, but they would ultimately have some influence on the detailed dynamics, because of the high degree of chaos that ultimately would reach halo scale.

4.2. Transportation infrastructure in galaxies, galaxy clusters, and cities

Coming back to questions raised in 1.1, can network theory help to understand implications of the difference in structure in high and low-mass halo root systems? The root systems are precisely external transport networks, carrying matter in from a uniform arrangement into haloes. This closely corresponds to a river network carrying rainwater that has fallen uniformly on a landscape, or the flow of food into a city along roads, imagining food to sprout nearly uniformly as well over a landscape.

After entering the halo, though, the various accretion streams (subhaloes) that comprised the root-system tree would interact at some level, some of them passing nearby or through each other, the gas perhaps forming shocks and dissipating energy. But many root-remnants would not interact; after all, hundreds of galaxies exist together in a galaxy-cluster halo. So, it is not so clear whether to consider the root system to be relevant to dynamics inside the halo.

In any case, how does the infrastructure scale with mass? (Mass seems to us to be the most obvious analog in a halo to a city’s population. Another possibility, for a halo with many galaxies or subhaloes, could be the number of these.) The seeming greater abundance and branching in large halo root systems suggests that their fractal dimension increases with halo mass, just as larger cities have street networks with larger dimensions (Shen 2002; Bettencourt 2021). If that translates into producing something more efficiently, what would that be?

Stars could be seen as ‘products’ of galaxies. But as we discussed in §3.2, a longtime observation in the field of galaxy formation is that star formation becomes *less*, not more efficient in high-mass haloes; this contradicts a naive prediction from city dynamics. We can interpret this consistently as follows: while the complex root structure might signal efficiency of total matter accretion, that infrastructure simply does not persist inside the halo. Or, cities are able to self-regulate adequately to translate efficient transport into high productivity, but there is no such self-regulation mechanism operating in a galaxy or halo. Other ‘products’ are possible in galaxies and haloes; the total energy dissipation, or some measure of entropy production, may not scale the same way as the star formation; we are not aware of a measurement of that. It would be interesting to measure this from simulations and test its scaling with halo mass.

Finally, we note that many of these systems relate to the problem of optimal transport, which has been applied in cosmology (Frisch *et al.* 2002; Levy *et al.* 2021), and in other systems (Peyré and Cuturi 2019), including city infrastructure (Leite and De Bacco 2024). In optimal transport, the path taken from source to destination is not always considered, but it has been found that branching structures can spontaneously emerge in an optimal transport problem (Facca *et al.* 2021), if an increase in flux through a certain patch increases a conductivity parameter through a medium. Assembly through these ‘roots’ appears to be the optimal way to assemble mass together through gravity, just as in so many other systems.

AUTHOR CONTRIBUTIONS

MN led, carried out the analysis, and wrote the paper, with essential contributions, including code, ideas, and figure edits, from MAC and IS.

ACKNOWLEDGMENTS

We thank the developers and maintainers of the IllustrisTNG database that enabled this work. MN thanks the organizers of the recent conferences ‘Mind the Gap: Galaxies and the Large-Scale Structure’ and ‘Cosmic Flows 2025’ for providing stimulating environments that encouraged the ideas and work presented here, and thanks Antonela Taverna for providing an in-preparation python implementation of the MMF. MAC acknowledges support from the Programa de Apoyo a Proyectos de Investigación e Innovación Tecnológica (PAPIT) IN115224 and CONAHCyT project CF-2023-I-1971. IS acknowledges NASA grants N4-ADAP24-0021 and 24-ADAP24-0074, and this research was supported in part by grant NSF PHY-2309135 to the Kavli Institute for Theoretical Physics (KITP); these also enabled a visit of MN to IS to work on this paper.

REFERENCES

- J. R. Bond, L. Kofman, and D. Pogosyan, *Nature* **380**, 603 (1996), [astro-ph/9512141](#).
- P. Ball, *Nature* **543**, 314 (2017).
- M. C. Neyrinck, J. Hidding, M. Konstantatou, and R. van de Weygaert, Royal Society Open Science, in press (2018), [arXiv:1710.04509](#).
- F. Vazza and A. Feletti, *Frontiers in Physics* **8**, 491 (2020).
- M. Neyrinck, T. Elul, M. Silver, E. Mallouh, M. Aragón-Calvo, S. Banducci, C. Bloyd, T. Boodhoo, B. Diemer, B. Falck, D. Feldman, Y. Chung Han, J. Kruk, S. J. Kwak, Y. Mungan, M. Novelo, R. Patel, P. Phanichphant, J. Primack, O. Sporns, F. Stearns, A. Victor, D. Weinberg, and N. M. Zahr, *arXiv e-prints*, [arXiv:2008.05942](#) (2020), [arXiv:2008.05942 \[physics.pop-ph\]](#).
- H. Cuntz, F. Forstner, A. Borst, and M. Häusser, *PLoS computational biology* **6**, e1000877 (2010).
- D. Leite and C. De Bacco, *Nature Communications* **15**, 7981 (2024).
- N. Tanabe, S. Sato, B. Suki, and T. Hirai, *Frontiers in Physiology* **11** (2020), [10.3389/fphys.2020.603197](#).
- C. Srisawat, A. Knebe, F. R. Pearce, A. Schneider, P. A. Thomas, P. Behroozi, K. Dolag, P. J. Elahi, J. Han, J. Helly, Y. Jing, I. Jung, J. Lee, Y.-Y. Mao, J. Onions, V. Rodriguez-Gomez, D. Tweed, and S. K. Yi, *MNRAS* **436**, 150 (2013), [arXiv:1307.3577 \[astro-ph.CO\]](#).
- R. B. Tully, H. Courtois, Y. Hoffman, and D. Pomarède, *Nature* **513**, 71 (2014), [arXiv:1409.0880 \[astro-ph.CO\]](#).
- A. Dupuy and H. M. Courtois, *A&A* **678**, A176 (2023), [arXiv:2305.02339 \[astro-ph.CO\]](#).
- A. Valade, N. I. Libeskind, D. Pomarède, R. B. Tully, Y. Hoffman, S. Pfeifer, and E. Kourkchi, *Nature Astronomy* **8**, 1610 (2024), [arXiv:2409.17261 \[astro-ph.CO\]](#).
- Y. Hoffman, A. Valade, N. I. Libeskind, J. G. Sorce, R. B. Tully, S. Pfeifer, S. Gottlöber, and D. Pomarède, *MNRAS* **527**, 3788 (2024), [arXiv:2311.01340 \[astro-ph.CO\]](#).
- G. West, *Scale: The Universal Laws of Growth, Innovation, Sustainability, and the Pace of Life in Organisms, Cities, Economies, and Companies* (Penguin Publishing Group, 2017).
- L. M. Bettencourt, *science* **340**, 1438 (2013).
- L. Bettencourt, *Introduction to Urban Science: Evidence and Theory of Cities as Complex Systems* (MIT Press, 2021).
- C. Alexander, *Architectural Forum* **122**, 58 (1965).
- T. Nozakura and S. Ikeuchi, *ApJ* **279**, 40 (1984).
- J. Hidding, “jhidding/nbody2d: 2d PM n-body code,” (2020).
- B. L. Falck, M. C. Neyrinck, and A. S. Szalay, *ApJ* **754**, 126 (2012), [arXiv:1201.2353](#).
- S. van der Walt, J. L. Schönberger, J. Nunez-Iglesias, F. Boulogne, J. D. Warner, N. Yager, E. Gouillart, T. Yu, and the scikit-image contributors, *PeerJ* **2**, e453 (2014).
- A. Pillepich, V. Springel, D. Nelson, S. Genel, J. Naiman, R. Pakmor, L. Hernquist, P. Torrey, M. Vogelsberger, R. Weinberger, and F. Marinacci, *MNRAS* **473**, 4077 (2018), [arXiv:1703.02970](#).
- D. Nelson, V. Springel, A. Pillepich, V. Rodriguez-Gomez, P. Torrey, S. Genel, M. Vogelsberger, R. Pakmor, F. Marinacci, R. Weinberger, L. Kelley, M. Lovell, B. Diemer, and L. Hernquist, *Computational Astrophysics and Cosmology* **6**, 2 (2019a), [arXiv:1812.05609 \[astro-ph.GA\]](#).
- D. Nelson, A. Pillepich, V. Springel, R. Pakmor, R. Weinberger, S. Genel, P. Torrey, M. Vogelsberger, F. Marinacci, and L. Hernquist, *MNRAS* **490**, 3234 (2019b), [arXiv:1902.05554 \[astro-ph.GA\]](#).
- Planck Collaboration, P. A. R. Ade, N. Aghanim, M. Arnaud, M. Ashdown, J. Aumont, C. Baccigalupi, A. J. Banday, R. B. Barreiro, J. G. Bartlett, and et al., *ArXiv e-prints* (2015), [arXiv:1502.01589](#).
- A. Heavens and J. Peacock, *MNRAS* **232**, 339 (1988).
- A. Knebe, S. R. Knollmann, S. I. Muldrew, F. R. Pearce, M. A. Aragón-Calvo, Y. Ascasibar, P. S. Behroozi, D. Ceverino, S. Colombi, J. Diemand, K. Dolag, B. L. Falck, P. Fasel, J. Gardner, S. Gottlöber, C.-H. Hsu, F. Iannuzzi, A. Klypin, Z. Lukić, M. Maciejewski, C. McBride, M. C. Neyrinck, S. Planelles, D. Potter, V. Quilis, Y. Rasera, J. I. Read, P. M. Ricker, F. Roy, V. Springel, J. Stadel, G. Stinson, P. M. Sutter, V. Turchaninov, D. Tweed, G. Yepes, and M. Zemp, *MNRAS* **415**, 2293 (2011), [arXiv:1104.0949](#).
- A. D. Ludlow and C. Porciani, *MNRAS* **413**, 1961 (2011), [arXiv:1011.2493 \[astro-ph.CO\]](#).
- D. Galárraga-Espinosa, E. Garaldi, and G. Kauffmann, *A&A* **671**, A160 (2023), [arXiv:2209.05495 \[astro-ph.GA\]](#).
- M. A. Aragón-Calvo, R. van de Weygaert, and B. J. T. Jones, *MNRAS* **408**, 2163 (2010a), [arXiv:1007.0742 \[astro-ph.CO\]](#).
- S. Moccia, E. De Momi, S. El Hadji, and L. S. Mattos, *Computer methods and programs in biomedicine* **158**, 71 (2018).
- M. A. Aragón-Calvo, B. J. T. Jones, R. van de Weygaert, and J. M. van der Hulst, *A&A* **474**, 315 (2007), [arXiv:0705.2072 \[astro-ph\]](#).
- M. C. Neyrinck, in *Origami⁶: Sixth International Meeting of Origami Science, Mathematics, and education*, edited by K. Miura, T. Kawasaki, T. Tachi, R. Uehara, R. Lang, and P. Wang-Iverson (2015) [arXiv:1408.2219](#).
- M. A. Aragón-Calvo, M. C. Neyrinck, and J. Silk, *arXiv e-prints*, [arXiv:1412.1119](#) (2014), [arXiv:1412.1119 \[astro-ph.GA\]](#).
- R. Weinberger, V. Springel, and R. Pakmor, *ApJS* **248**, 32 (2020), [arXiv:1909.04667 \[astro-ph.IM\]](#).
- S. Genel, M. Vogelsberger, D. Nelson, D. Sijacki, V. Springel, and L. Hernquist, *MNRAS* **435**, 1426 (2013), [arXiv:1305.2195 \[astro-ph.IM\]](#).
- M. A. Aragón Calvo, M. C. Neyrinck, and J. Silk, *The Open Journal of Astrophysics* **2**, 7 (2019), [arXiv:1607.07881 \[astro-ph.GA\]](#).
- S. Genel, G. L. Bryan, V. Springel, L. Hernquist, D. Nelson, A. Pillepich, R. Weinberger, R. Pakmor, F. Marinacci, and M. Vogelsberger, *ApJ* **871**, 21 (2019), [arXiv:1807.07084](#).
- M. Neyrinck, S. Genel, and J. Stücker, *arXiv e-prints*, [arXiv:2206.10666](#) (2022), [arXiv:2206.10666 \[physics.hist-ph\]](#).
- B. Moore, S. Ghigna, F. Governato, G. Lake, T. Quinn, J. Stadel, and P. Tozzi, *ApJ* **524**, L19 (1999), [astro-ph/9907411](#).
- G. F. R. Ellis and W. R. Stoeger, *MNRAS* **398**, 1527 (2009), [arXiv:1001.4572 \[astro-ph.CO\]](#).

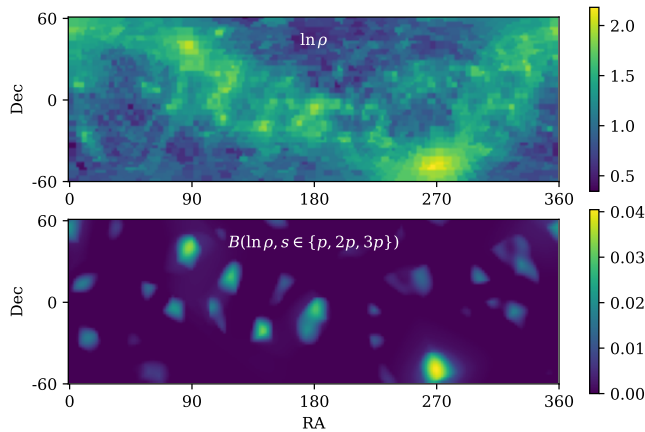


FIG. 5.— An example ‘blobbiness’ field, measured from the log-density in a spherical shell of a halo root system. We looked for blobs at three scales (1, 2, and 3 times the scale size in degrees p of a pixel at radius r), combining into a multiscale-blob field.

- D. Bandak, A. A. Mailybaev, G. L. Eyink, and N. Goldenfeld, *Phys. Rev. Lett.* **132**, 104002 (2024), arXiv:2401.13881 [physics.flu-dyn].
- M. C. Neyrinck, *MNRAS* **452**, L26 (2015b), arXiv:1409.0057 [astro-ph.CO].
- G. Shen, *International Journal of Geographical Information Science* **16**, 419 (2002).
- U. Frisch, S. Matarrese, R. Mohayaee, and A. Sobolevski, *Nature* **417**, 260 (2002), arXiv:astro-ph/0109483 [astro-ph].
- B. Levy, R. Mohayaee, and S. von Hausegger, *MNRAS* **506**, 1165 (2021), arXiv:2012.09074 [astro-ph.CO].
- G. Peyré and M. Cuturi, *Foundations and Trends® in Machine Learning* **11**, 355 (2019).
- E. Facca, F. Cardin, and M. Putti, *Journal of Computational Physics* **447**, 110700 (2021).
- A. F. Frangi, W. J. Niessen, K. L. Vincken, and M. A. Viergever, in *Medical image computing and computer-assisted intervention—MICCAI’98: first international conference cambridge, MA, USA, october 11–13, 1998 proceedings 1* (Springer, 1998) pp. 130–137.
- M. A. Aragón-Calvo, R. van de Weygaert, and B. J. T. Jones, *MNRAS* **408**, 2163 (2010b), arXiv:1007.0742 [astro-ph.CO].

APPENDIX

To quantify root abundance in the root system, we count blobs using a 2D Hessian-based blob filter, applied to a spherical shell of radius r around the halo root system centroid. It is a similar method to one introduced to bring out multiscale features resembling blood vessels by Frangi *et al.* (1998), but instead is tuned to find (smeared) pointlike blobs; it is the node-finding part of Aragón-Calvo *et al.* (2010b)’s Multiscale Morphology Filter (MMF).

The Hessian-based blob filter works on a field ρ smoothed on a scale s , $G(\rho, s)$. At a single scale s , it returns the magnitude of the smallest eigenvalue of the Hessian matrix of the image, where that eigenvalue is negative; otherwise, zero:

$$B(\rho, s) = |e_0(G(\rho, s))|(e_0(\rho, s) < 0). \quad (1)$$

where e_0 is the smallest eigenvalue of the Hessian of the field. The final multiscale filter is the maximum of this field over several measured scales.

We used the simple equirectangular projection to translate right ascension and declination on the shell onto a grid, padding the edges substantially to avoid edge effects, and using only declination between -60 and 60 because of the distortion at the poles. To cover the rest of the spherical shell, we measured B from two other rotations of the halo root system, and took the median of the average blobbiness fields among the three rotations.

Fig. 5 shows a spherical shell through the cubic grid, for halo 40, and at a radius 15 voxels away from the center, and the multiscale ‘blobbiness’ field B . The pixelation of the grid, and its distortion from the spherical projection, is visible at top. The smoothing scales we used in the filter were 1, 2, and 3 times the pixel scale, i.e. the angular size of a pixel a distance r away from the center, at the equator.

There is substantial room for improvement in this root-finding method, but we would like to think this is adequate for a first quantification of them. Ultimately, we would like to map the roots as has been done in other vascular systems. Some discussion of the challenges and further ideas for quantifying them is in the main text.